Collection SFN **12** (2011) 233–245

DOI: 10.1051/sfn/201112011

A comparative thermodynamic and structural investigation of $Ge_xTe_{(1-x)}$ and $Ge_xSb_yTe_{(1-x-y)}$ liquid alloys

C. Otjacques[1], J.-Y. Raty[1], J.-P. Gaspard[1], Y. Tsuchiya[2] and C. Bichara[3]

[1]*Physique de la Matière Condensée, B5, Université de Liège, 4000 Sart-Tilman, Belgium*
[2]*Department of Physics, Faculty of Science, Niigata University, Ikarashi 2-8050, Niigata 950-2181, Japan*
[3]*Centre Interdisciplinaire de Nanoscience de Marseille, CINaM CNRS and Aix-Marseille Universities, Campus de Luminy, Case 913, 13288 Marseille, France*

Abstract. Thermodynamic properties (density and sound velocity) of liquid $GeSb_2Te_4$ and $Ge_2Sb_2Te_5$ alloys have been measured and compared with previously published data on $Ge_{0.075}Te_{0.925}$ and $Ge_{0.15}Te_{0.85}$ alloys that display a negative thermal expansion (NTE) in the liquid state. This comparison is extended to the analysis of their structural and dynamical properties investigated by neutron scattering measurements performed on the D4 and IN6 spectrometers at the ILL (Grenoble). These experimental results, complemented by First Principles Molecular Dynamics simulations of the liquids, lead us to propose a model for the density anomaly observed in some of these tellurium based systems, when they are not too dense: it corresponds to a structural change between a low temperature liquid, characterized by a low density and an octahedral local order distorted by a Peierls-like distortion mechanism, and a high temperature liquid in which the vibrational entropy gain favors a more symmetric (less distorted) octahedral local order.

1. INTRODUCTION

Some liquid tellurium based alloys such as HgTe [1, 2], In_2Te_3 [3], Ga_2Te_3 [3], As_2Te_3 [4] as well as Ge_xTe_{1-x} with $(0 \leq x \leq 0.2)$ [5–7] display a Negative Thermal Expansion (NTE), meaning that their volume contracts upon heating. For the latter system, the temperature range of the NTE is of the order of 100 K above the eutectic point or liquidus line, in the thermodynamic equilibrium state, or in the undercooled liquid state. This unusual thermodynamic behavior is also observed in water, between 273 and 277 K [8] and, as discussed by Barrera et al. [9], in a number of solids with different types of structures and different bonding mechanisms : in alkali halides with rocksalt structure, in semiconductors with zinc blende structure, or in more complex structures made of rigid units bonded through bridging atoms.

In the tellurium based systems investigated here, the bonding results from the overlap of p orbitals, with a limited role played by the sp hybridization and the ionicity difference between the elements. A systematic investigation of the liquid structure [10] showed that, for average numbers of p electrons larger than 4.5, distorted octahedral structure are favored. The structural changes are then essentially driven by a Peierls-like distortion mechanism that has been shown to act also on disordered systems because the electronic structure essentially depends on the local order [11–14].

In this paper, we focus on $Ge_xTe_{(1-x)}$ and $Ge_xSb_yTe_{(1-x-y)}$ liquid alloys. We first present density and sound velocity measurements that clearly show the specific and unusual behavior of the $Ge_xTe_{(1-x)}$ alloys as opposed to the alloys containing antimony that, in their solid (amorphous or crystalline) state, are used as active material for the so called 'Phase Change' non volatile data storage systems [15].

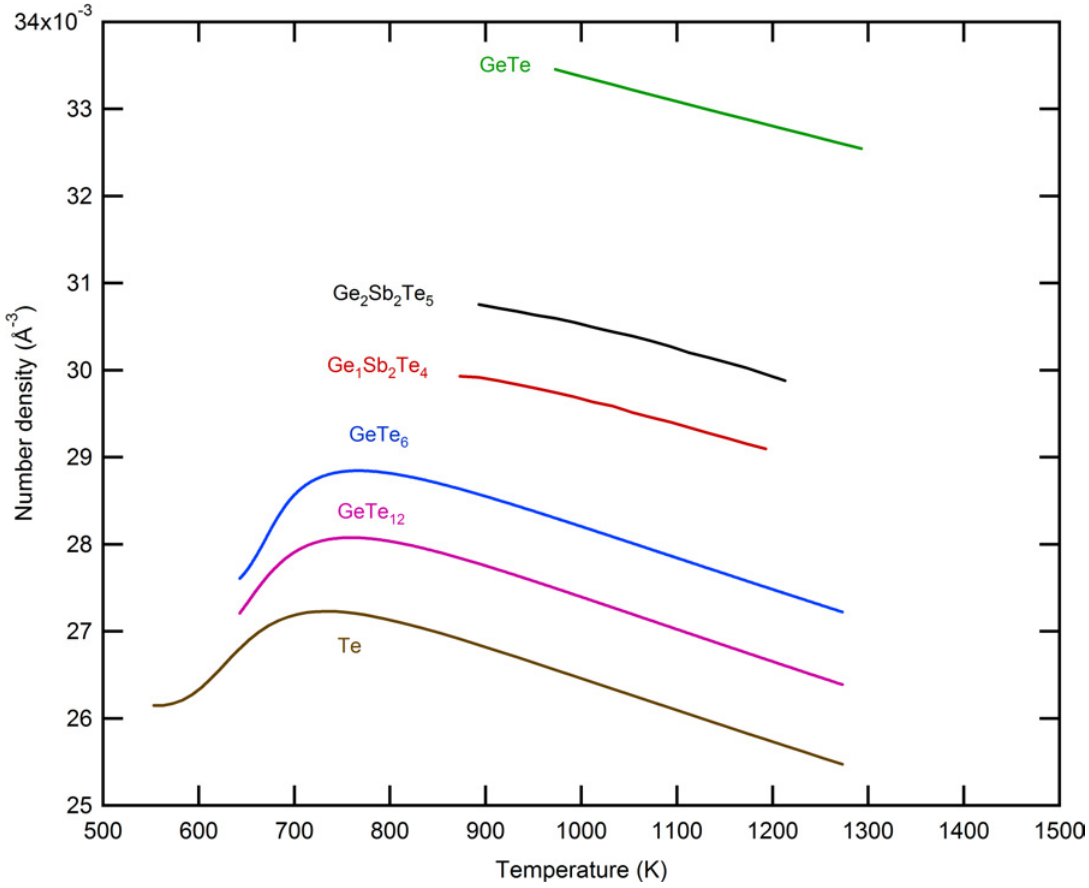

Figure 1. Number density of liquid $Ge_xSb_yTe_{(1-x-y)}$ alloys.

We then try to understand the microscopic origin of this Negative Thermal Expansion by investigating the liquid structure and its dynamics by neutron scattering. Finally we use First Principles Molecular Dynamics (FPMD) to help interpreting these data and give a microscopic view of the mechanisms that drive the structure and thermodynamic properties of these systems.

2. DENSITY AND SOUND VELOCITY MEASUREMENTS

The densities of liquid $Ge_1Sb_2Te_4$ and $Ge_2Sb_2Te_5$, have been newly measured using the γ-ray attenuation method described in [16]. Data on liquid GeTe, $Ge_{0.15}Te_{0.85}$ (denoted $GeTe_6$ in the following), $Ge_{0.075}Te_{0.925}$ (denoted $GeTe_{12}$ in the following) and pure Te have been added for the sake of comparison. The density of $GeTe_6$ and $GeTe_{12}$ has been evaluated by interpolation using the data for 6 specimens between Te and 15 at% of Ge [17]. Firstly the molar volume as a function of temperature was fitted to a smooth curve using an inhomogeneous structure model [18]. Secondly the respective parameters for the inhomogeneous model as a function of Ge concentration were interpolated to $GeTe_6$ and $GeTe_{12}$. In figure 1, we clearly see that $Ge_xTe_{(1-x)}$ (with $0 \leq x \leq 0.15$) alloys are less dense than GeTe and $Ge_2Sb_2Te_5$. In addition, between 600 and 733 K, depending of the composition, the density of these liquids increases by about 5%.

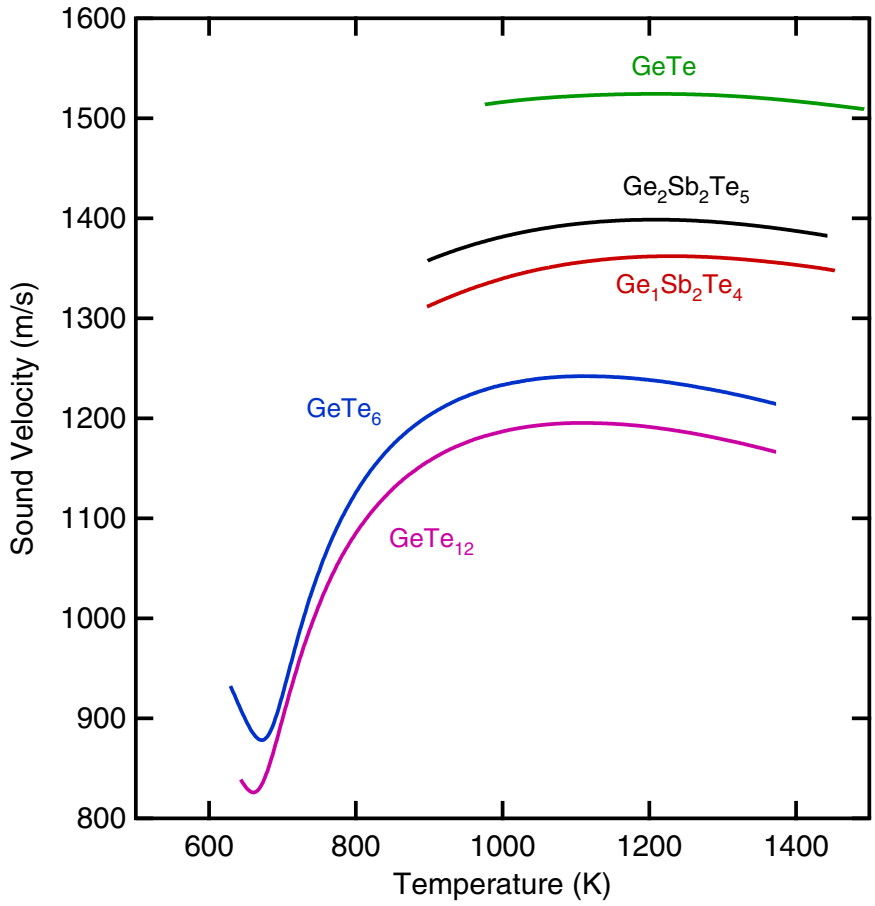

Figure 2. Sound velocity in liquid $Ge_xSb_yTe_{(1-x-y)}$ alloys.

The same spectacular behavior is observed on the sound velocities data that have been measured using the standard pulse echo overlap technique described in [19]. They are plotted in Figure 2. As expected for a more dense liquid, the sound velocities of GeTe, $Ge_2Sb_2Te_5$, and $Ge_1Sb_2Te_4$ are larger than for $Ge_xTe_{(1-x)}$ $(0 \leq x \leq 0.15)$ alloys. They are almost constant, with a tendency to decrease at higher temperatures, although their density constantly decreases. In $GeTe_6$ and $GeTe_{12}$ though, a dramatic increase of the sound velocity, by about 30% in a 300 K temperature interval, is observed, obviously coupled with the negative thermal expansion.

Sound velocity measurements turn out to be a very sensitive probe of the structural changes that take place in the liquid. This behavior has to be related with the specific heat change, measured in [20]: the sharply peaked heat capacities are also indicative of a strong change in the liquid structure. These latter data are indeed of great value since, by integrating Cp/T as a function of temperature, one has access to the total entropy change in the liquid that can be related to the changes in the vibrational densities of states.

3. NEUTRON SCATTERING EXPERIMENT

We performed neutron scattering experiments on the two-axis D4 diffractometer, on $Ge_{0.15}Te_{0.85}$ and $Ge_{0.075}Te_{0.925}$. Samples were prepared from the pure elements, molten, homogenized and then sealed under vacuum in quartz tubes of 6 mm internal/8 mm external diameter. Special care was taken to

Table 1. Experimental densities at temperatures studied by neutron scattering for $GeTe_6$ and $GeTe_{12}$.

$GeTe_6$		$GeTe_{12}$	
T(K)	ρ (at/Å^{-3})	T(K)	ρ (at/Å^{-3})
623	0.02755	673	0.02771
643	0.02769	693	0.02792
653	0.02780	723	0.02809
685	0.02839	758	0.02814
796	0.02888	813	0.02808

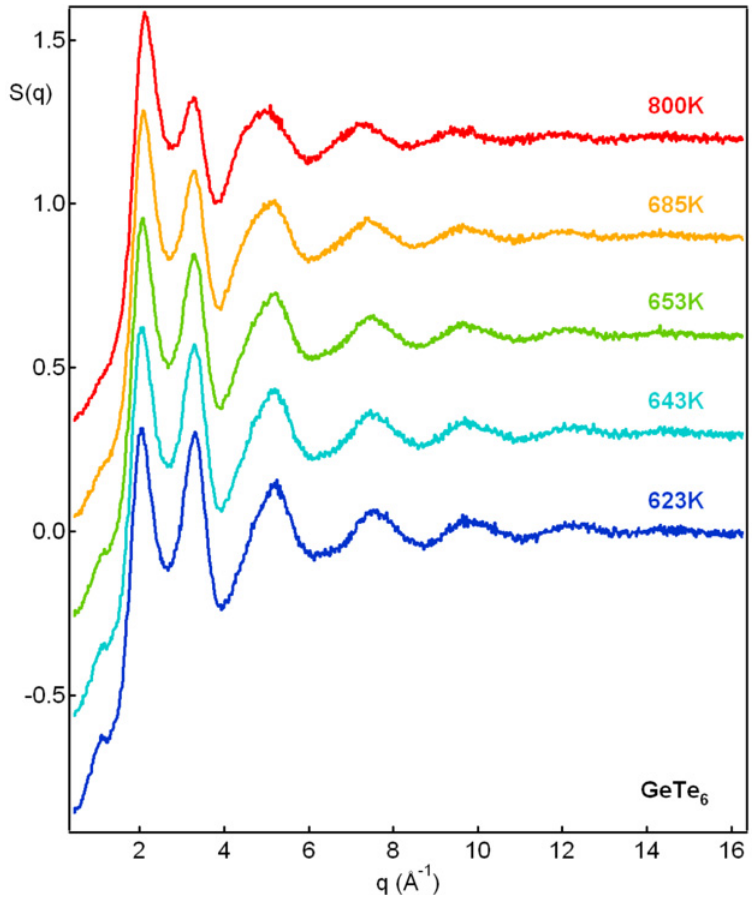

Figure 3. Temperature evolution of the static structure factor $S(q)$ of $GeTe_6$ liquid alloy measured on the D4 spectrometer at ILL.

limit the empty volume inside the container as Te high vapor pressure could cause significant variations in composition with temperature. The total scattered intensity was measured for an incident neutron wavelength $\lambda = 0.6956$. The 2θ angular range extended from 0.750° up to 138.5° with a 2θ step equal to 0.125° which corresponds to neutron scattering vectors $q = 4\pi \sin\theta/\lambda$ in the range 0.118 to 16.893 Å^{-1}. The temperatures at which the total static structure factor was measured and the corresponding densities are given in table 1.

The structure factors, $S(q)$, of $GeTe_6$ and $GeTe_{12}$ are presented in Figures 3 and 4 respectively. We can see well resolved oscillations up to a maximal q of 16 Å^{-1}. The changes with T are more noticeable

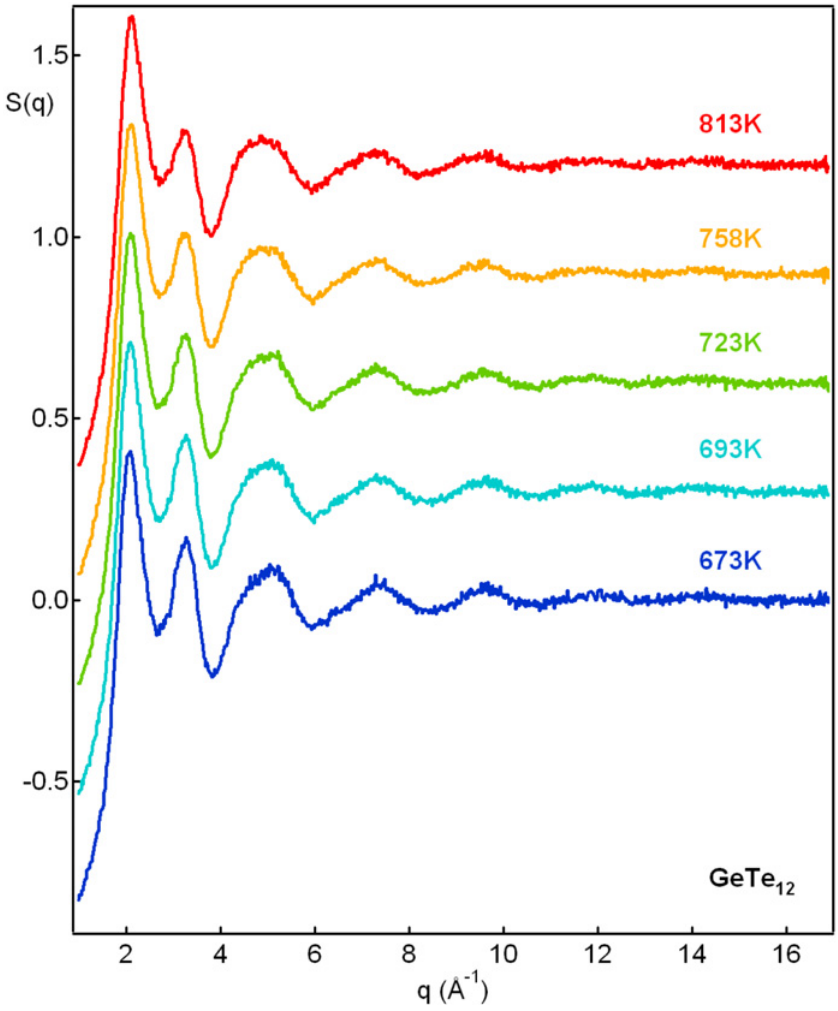

Figure 4. Temperature evolution of the static structure factor $S(q)$ of $GeTe_{12}$ liquid alloy measured on the D4 spectrometer at ILL.

Table 2. Changes (in %) in height (ΔH/H) and position (Δq/q, in $Å^{-1}$) of the three first peaks of $S(q)$, between lowest and highest T, for $GeTe_6$ and $GeTe_{12}$.

Compound	peak 1		peak 2		peak 3	
	ΔH/H	Δq/q	ΔH/H	Δq/q	ΔH/H	Δq/q
$GeTe_6$	+6.1%	+4.4%	−13%	−1.2%	−6%	−5.3%
$GeTe_{12}$	+0.7%	+1.9%	−6.8%	−1.1%	+0.9%	−2.4%

in the case of $GeTe_6$: a strong evolution of $S(q)$ is observed, with a decrease of second and third peak heights. These evolutions and the peak positions are in agreement with the results reported in [21]. In $GeTe_{12}$, the same tendency is observed, to a lesser extent: the measurements have been made at higher T compared to the NTE range because of the experimental impossibility to reach lower T. The changes in height and position of the three first peaks of $S(q)$, between lowest and highest T, for both compounds, are reported in Table 2. We see that the largest evolution, in both compounds, is the decrease of second

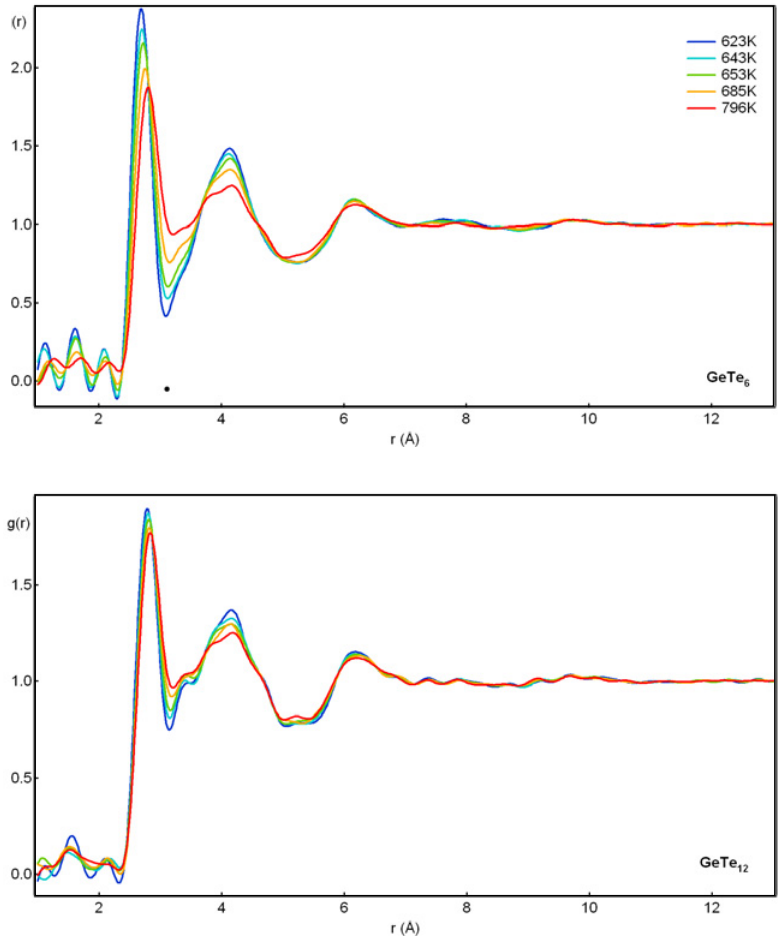

Figure 5. Pair correlation functions obtained at different temperatures for (upper panel) $GeTe_6$ and (lower panel) $GeTe_{12}$.

Table 3. Positions (in Å), of the three first peaks of $g(r)$, at lowest and highest T, for $GeTe_6$ and $GeTe_{12}$.

Compound	T (K)	peak 1	peak 2	peak 3
$GeTe_6$	623	2.69	4.14	6.16
	796	2.81	4.16	6.18
$GeTe_6$ [21]	633	2.68	4.12	6.17
	943	2.86	4.12	6.26
$GeTe_{12}$	673	2.79	4.17	6.18
	813	2.83	4.18	6.20

peak height with T. In $GeTe_6$, we also observe a decrease of the third peak height and an increase of the first peak height, while in $GeTe_{12}$ both remain more or less constant. The peak's positions are evolving with T, specially in $GeTe_6$, where the first peak is shifted to larger q while the second and third are shifted to smaller q.

The pair correlation functions $g(r)$, presented in Figure 5, were obtained by Fourier transformation of the $S(q)$ without the use of a damping function. When temperature increases, the position of the

first peak slightly shifts to higher r values while the positions of the following peaks remain more or less constant (see Table 3), and their heights decrease. Between the lowest and highest temperatures, the coordination numbers calculated by integrating the first peak of $g(r)$ up to a cut off distance r_{cut} evolve from 2.4 to 2.9 in $GeTe_6$ ($r_{cut} = 3.10$ and 3.24 Å) and from 2.3 to 2.6 in $GeTe_{12}$ ($r_{cut} = 3.16$ and 3.22 Å). These coordination numbers are in agreement with the results in [21] for liquid $GeTe_6$.

These new data, that confirm the previously published neutron scattering results on $GeTe_6$ [21] indicate that both $GeTe_6$ and $GeTe_{12}$ undergo strong structural changes in the NTE temperature range.

4. INELASTIC SCATTERING EXPERIMENT

We measured the dynamical structure factor $S(2\theta, \omega)$ for $GeTe_6$, $GeTe_{12}$, $Ge_1Sb_2Te_4$ and $Ge_2Sb_2Te_5$ at various temperatures by neutron inelastic scattering on the IN6 time-of-flight spectrometer (ILL, Grenoble). For $GeTe_6$, measurements were performed at 673, 773 and 873 K. For $GeTe_{12}$ they were made at 643, 683, 693, 703, 763 and 873 K. For $Ge_1Sb_2Te_4$ and $Ge_2Sb_2Te_5$ the temperatures were 973, 1073 and 1173 K. Samples were conditioned in the same way as for the D4 experiment, using quartz tubes of 8/10 mm diameter. We used a wavelength $\lambda = 4.1$ Å, which, together with a 2θ range ranging from 10 to 115°, gives access to a q range of 0.3 to 2.6 $Å^{-1}$. Because of the dominant scattering from the container, long counting times (minimum 5 hours) were required in order to obtain reasonable statistics on the final spectra. The quartz contribution to the signal was subtracted using a reference empty quartz tube, measured under the same conditions as the samples. By integrating $S(2\theta, \omega)$ over the 2θ range accessible to the experiment (10° to 115°) the vibrational density of states VDOS, $n(\omega)$ was obtained [22] and normalized to unity. As the q-range available to the experiment is finite and correlated with the ω range, the $n(\omega)$ density is incomplete and slightly distorted. However, since the (q, ω) range is the same for all measurements, comparisons of $n(\omega)$ are meaningful.

The measured VDOS's are presented in Figure 6. Overall they are quite similar for the four systems studied, with noticeable contributions up to ~40 meV and a main broad peak around 10–20 meV. Close to zero energy transfer, the full contribution of the quasielastic neutron scattering (QENS) due to diffusion in the liquid could be removed, while it still contributes at higher energies. For this reason, the VDOS increase steeply (almost linearly) at low energies. This effect is stronger at higher temperature for $GeTe_x$ and independent of T for PC materials. This indicates a strong variation in the diffusion coefficient in $GeTe_x$ within the NTE range and no significant variation in GST. Most importantly, contrasted results are clearly visible concerning the temperature dependence of the VDOS. The $Ge_1Sb_2Te_4$ and $Ge_2Sb_2Te_5$ VDOS's remain essentially unchanged in the 200 K range spanned. On the contrary, $GeTe_6$ and $GeTe_{12}$ VDOS's display a significant change with temperature. Between 18 and 35 meV, the vibrational modes are shifted towards lower energies (or frequencies) when temperature is increased within the range of the NTE. This red shift is thus related to the structural changes that are associated to the density anomaly. The softer vibrational modes at higher temperature give rise to a larger vibrational entropy. As shown in [23] this vibrational contribution amounts to about 60% of the total entropy variation calculated by integrating the heat capacity data.

5. FIRST PRINCIPLES MOLECULAR DYNAMICS

In order to gain an insight in the mechanisms driving the NTE in $GeTe_6$ at the atomistic level, we performed First Principles Molecular Dynamics simulations (FPMD) on a 216 atoms box (31 Ge and 185 Te) at the experimental liquid densities ($\rho = 0.02780\ Å^{-3}$ at 653 K, $\rho = 0.02819\ Å^{-3}$ at 673 K, $\rho = 0.02871\ Å^{-3}$ at 873 K). For the sake of comparison, we also simulated liquid $Ge_2Sb_2Te_5$ in a 162 atoms box (36 Ge, 36 Sb, 90 Te) at the experimental liquid density ($\rho = 0.0305\ Å^{-3}$). We first heated the liquid at 3000 K for 10 ps and then thermalized it at the requested temperatures for at least 10 ps each. We used the PW91 exchange correlation functional [24], ultrasoft pseudopotentials [25], Ge (4s and 4p)

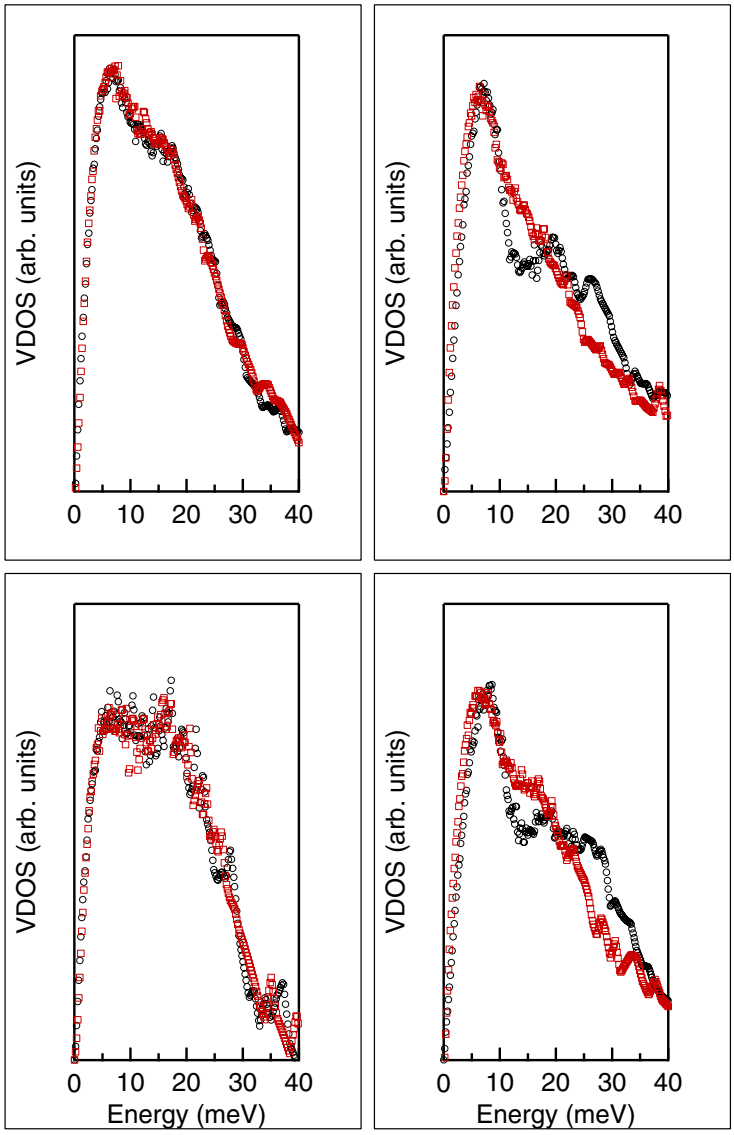

Figure 6. Vibrational densities of states (VDOS) measured on IN6 (ILL). Bottom left : $Ge_1Sb_2Te_4$. Black circles 973 K, red squares : 1173 K. Top left : $Ge_2Sb_2Te_5$. Black circles 973 K, red squares : 1173 K. Bottom right : $GeTe_6$. Black circles 673 K, red squares : 873 K. Top right : $GeTe_{12}$. Black circles 643 K, red squares : 873 K.

and Sb and Te (5s and 5p) valence electrons and a planewave cutoff energy of 175 eV. Calculations were performed at the Γ point only.

The structure factors, $S(q)$, calculated from the FPMD trajectories are presented in Figure 7, together with the experimental results under similar temperature conditions. At large q, the overall shape of experimental $S(q)$ is well reproduced by the simulations. At smaller q, the evolution of the two first peaks shows the same tendency as in the experiment: the height of first peak increases with T ($+8.2\%$) while for the second peak it decreases (-6.3%).

Nevertheless, the calculated $S(q)$ show peaks positions at lower q than the experimental ones, which leads to a slight overestimation of the distances in the calculated $g(r)$ displayed in Figure 8, and to

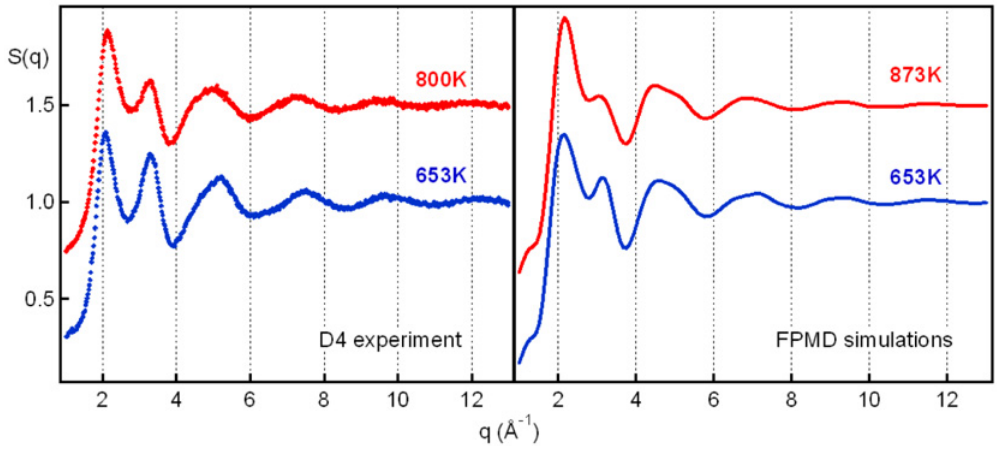

Figure 7. Temperature evolution of the total structure factor $S(q)$ of liquid $GeTe_6$: experimental (left panel) and FPMD results (right panel). High temperature curves are y-shifted by 0.5.

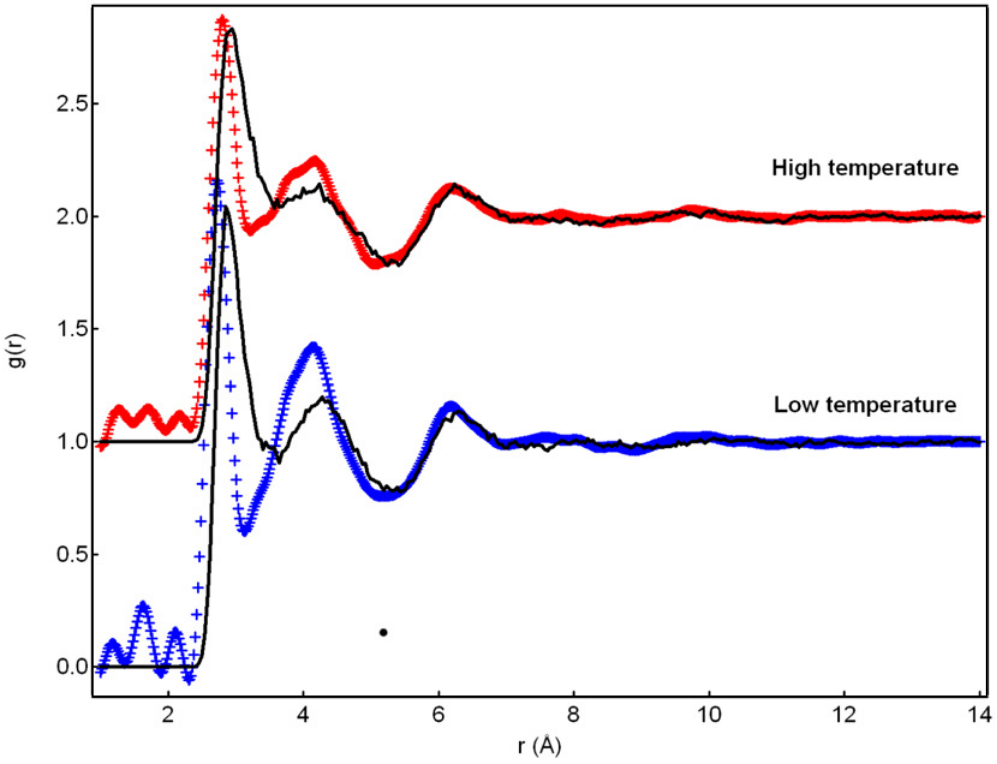

Figure 8. Pair correlation functions of liquid $GeTe_6$ at high and low temperatures, from experiment (markers) and FPMD (black lines). High temperature curves are y-shifted by 1.

an underestimation of vibrational frequencies. This has been observed previously for pure Te [26] or Te-rich alloys [12] and is due to the GGA approximation which slightly overestimates the Te-Te bond lengths and does not correctly account for the short long splitting of the neighbor distances in the first coordination shell. Calculated partial pair correlation functions are shown in Figure 9 and partial

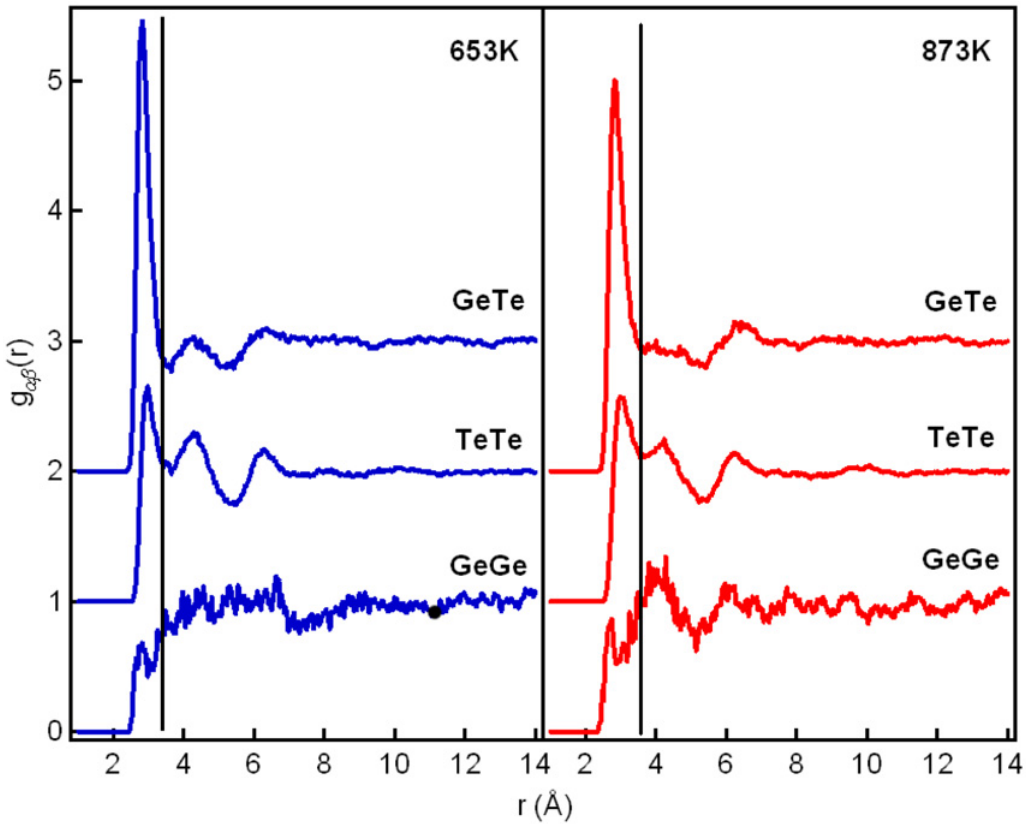

Figure 9. Partial pair correlation functions of liquid $GeTe_6$ at high and low temperatures. The vertical black lines indicate the cutoff distances taken to compute the coordination numbers.

Table 4. Positions of the first minimum r_{min}^{fpmd} (taken as the cutoff distance for integration) in total pair correlation functions, $g(r)$ (from FPMD), partial coordination numbers from partial pair correlation functions, $g_{\alpha\beta}(r)$, and total coordination numbers for Ge and Te atoms. Distances are given in Å.

T (K)	r_{min}^{fpmd}	N_c^{GeGe}	N_c^{GeTe}	N_c^{TeGe}	N_c^{TeTe}	N_c^{Ge}	N_c^{Te}
653	3.40	0.2(3)	4.3(6)	0.7(3)	2.5(8)	4.5(9)	3.3(1)
873	3.56	0.3(7)	4.9(9)	0.8(3)	3.4(4)	5.3(6)	4.2(7)
680 [28]	3.46	0.2	3.6	0.6	2.5	3.8	3.1

coordination numbers are given in table 4. The coordination numbers around Ge and Te are larger than what was found in [27] because of the clear overestimation of the widths of the first peaks of $g(r)$ in the simulations (see Figure 8). However, their temperature evolution (about $+1$ neighbor around Ge and Te in $\simeq 200$ K) is quite similar.

6. DISCUSSION

The evidences gathered from thermodynamic measurements, structural investigations and computer simulations can be understood in terms of a liquid structure model. The paradigm here is the the $\alpha \rightarrow \beta$

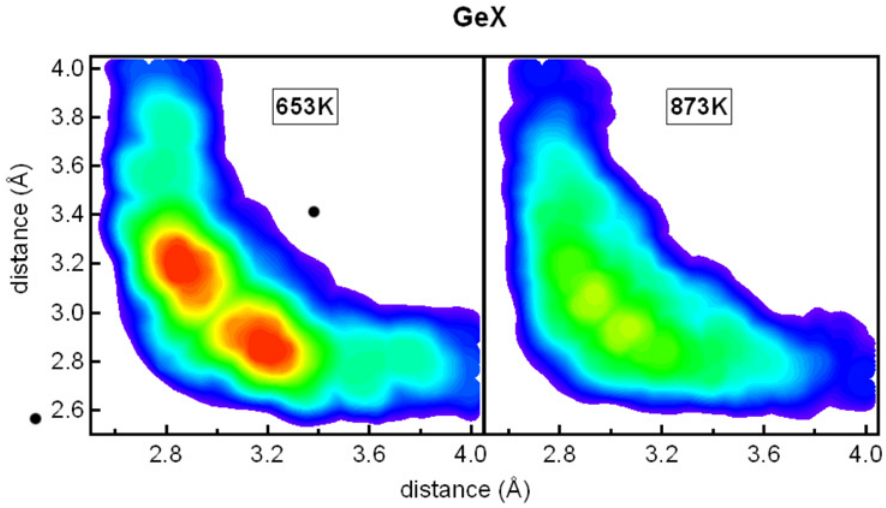

Figure 10. Three body correlation functions for almost aligned triplets of atoms, centered on Ge atoms, calculated on simulated $GeTe_6$ structures, at 653K (left panel) and 873K (right panel). Contours are drawn between 35% of the maximum value and maximum value of normalized correlation at 653 K (from blue to red).

transition of the crystalline GeTe compound that takes place around 700 K [29]. It is generally seen as a transition from a Peierls distorted low temperature phase (α, rhombohedral, a binary analogue of grey arsenic structure A7) to an almost cubic (β, NaCl-type) phase. At the transition, the molar volume shrinks by about 1%, shorter GeTe bonds elongate and longer ones shrink. Since the octahedral symmetry of the atomic environment is essentially preserved, along the (100) directions one has a short-long bond alternation in the α phase, while in the β phase, all successive bond lengths are equal. We can probe the same kind of three body correlation in the liquid state, before and just after the NTE by analyzing the correlations between 'almost' (i.e. : forming bond angles larger than 165°) aligned bonds, to take into account the inherent disorder of the liquid. This is presented in Figure 10. We see that in the low temperature, less dense, liquid shorter and longer bonds alternate around Ge atoms. The same is observed around Te atoms. After the NTE, in the more dense liquid, this short long correlation is blurred or vanishing.

Having understood the structural change involved in the NTE, one may ask about its driving force. The inelastic neutron scattering measurements presented in section 4, together with the analysis of the vibrational entropy contribution discussed in [23] provide the answer. The low temperature liquid phase is stabilized by the Peierls distortion mechanism leading to the symmetry breaking of the local octahedral environment of each atom. Since short and strong bonds are formed, the vibrations are hindered and the reticulated liquid is indeed very viscous [30]. At the crossover, the local structure changes, short bonds elongate and, as indicated by the red-shift in the VDOS's, become weaker. The driving force is the gain in vibrational entropy that balances the loss of the internal energy gained by distortion at lower temperatures.

We also understand why the NTE behavior is not seen in the liquid PC-materials investigated here. Since they are significantly more dense than the $Ge_xTe_{(1-x)}$ alloys, the distortion of the local environment is less pronounced. As discussed in [11], such a distortion results from a gain in electronic energy by opening a gap or a pseudo gap at the Fermi level in the electronic density of states, that is balanced by the repulsive energy cost of the distortion. In a more dense liquid, the latter term becomes more important and the distortion is weaker or vanishing.

7. CONCLUSION

By putting together new thermodynamic measurements (density, sound velocity), structural and vibrational experimental investigations by neutron scattering and computer simulations by FPMD, on some $Ge_xTe_{(1-x)}$ and $Ge_xSb_yTe_{(1-x-y)}$ liquid alloys, we could gain a better understanding of the origin of the negative thermal expansion observed in some of these liquids. As opposed to the well documented case of water that involves modifications of the packing of tetrahedral units, the negative thermal expansion in this system results from an original mechanism. It consists of a structural change between a low temperature liquid, characterized by a low density and an octahedral local order distorted by a Peierls-like distortion mechanism, and a high temperature liquid in which the vibrational entropy gain favors a more symmetric (less distorted) octahedral local order. Through this model we understand why this NTE is accompanied by an increase of the number of neighbors, a rather unusual behavior in a standard liquid. Our data give no evidence for a NTE in the equilibrium liquid state of the liquid PC-materials investigated. This possibility cannot be ruled out in an hypothetical undercooled liquid state, but is rather unlikely, due to the larger density of these systems. However, the underlying physics, driven by the more or less pronounced distortion of octahedral environments, certainly plays a major role in these systems.

References

[1] D. Chandra and L. R. Holland. *J. Vac. Sci. Technol. A*, 1:1620, 1983.
[2] D. Chandra. *Phys. Rev. B*, 31:7209, 1985.
[3] V. M. Glazov, S. N. Chizevskaya, and N. N. Glagoleva. *Liquid Semiconductors*. Plenum, New York, 1969.
[4] Y. Tsuchiya. *J. Non-Cryst. Solids*, 250-252:473–477, 1999.
[5] Y. Tsuchiya. *J. Phys. Soc. Jap.*, 60:227–34, 1991.
[6] Y. Tsuchiya. *Thermochimica Acta*, 314:275–280, 1998.
[7] H. Thurn and J. Ruska. *J. Non-Cryst. Solids*, 22:331, 1976.
[8] P. G. Debenedetti. *J. Phys. : Condens. Matter*, 15:R1669–1726, 2003.
[9] G.D. Barrera, J.A.O. Bruno, T.H.K. Barron, and N. L. Allan. *J. Phys.: Condens. Matter*, 17:R217–R252, 2005.
[10] C. Steimer, M.-V. Coulet, W.Welnic, H. Dieker, R. Detemple and C. Bichara, B. Beuneu, J.P. Gaspard, and M.Wuttig. *Advanced Mat.*, 20:4535–4540, 2008.
[11] J.-P. Gaspard, A. Pellegatti, F. Marinelli, and C. Bichara. *Philos. Mag. B*, 77:727, 1998.
[12] C. Bichara, M. Johnson, and J.-Y. Raty. *Phys. Rev. Lett.*, 95:267801, 2005.
[13] G. Zhao, C. S. Liu, Y. N. Wu, E. G. Jia, , and Z. G. Zhu. *Phys. Rev. B*, 74:184202, 2006.
[14] C. Bichara, M. Johnson, and J.-P. Gaspard. *Phys. Rev. B*, 75:060201(R), 2007.
[15] S. Raoux and M. Wuttig, editors. *Phase Change Materials: Science And Applications*. Springer, 2008.
[16] Y. Tsuchiya. *J. Phys. Soc. Jpn*, 57:3851–3857, 1988.
[17] Y. Tsuchiya. *J. Non-Cryst. Solids*, 312-314:212–216, 2002.
[18] Y. Tsuchiya and E. F. W. Seymour. *J. Phys. C: Solid State Phys.*, 18:4721–4734, 1985.
[19] Y. Tsuchiya and M. Hisakabe. *J. Non-Cryst. Solids*, 353:3000–3004, 2007.
[20] R. Castanet and C. Bergman. *Phys. Chem. Liq.*, 14:219, 1985.
[21] C. Bergman, C. Bichara, J.-P. Gaspard, and Y. Tsuchiya. *Phys. Rev. B*, 67:104202, 2003.
[22] D. Richard et al. Lamp, the large array manipulation program. `http://www.ill.eu/ instruments-support/computing-for-science/cs-software/all-software/lamp/`.

[23] C. Otjacques, J.-Y. Raty, M.-V. Coulet, M. Johnson, H. Schober, C. Bichara, and J.-P. Gaspard. *Phys. Rev. Lett.*, 103:245901, 2009.
[24] J. Perdew, J. A. Chevary, S. H. Vosko, K. A. Jackson, M. R. Pederson, D. J. Singh, and C. Fiolhais. *Phys. Rev. B*, 46:6671–6687, 1992.
[25] D. Vanderbilt. *Phys. Rev. B*, 41:7892, 1990.
[26] R. Stadler and M. J. Gillan. *J. Phys. Condens. Matter*, 12:6053, 2000.
[27] M.-V. Coulet, D. Testemale, J.-L. Hazemann, J.-P. Gaspard, and C. Bichara. *Phys. Rev. B*, 72:174209, 2005.
[28] J. Akola and R. O. Jones. *Phys. Rev. Lett.*, 100:205502, 2008.
[29] T. Chattopadhyay, J. X. Boucherle, and H. G. von Schnering. *J. Phys. C: Solid State Phys.*, 20:1431–1440, 1987.
[30] F. Herwig and M. Wobst. *Z. Metallkunde*, 83:35–39, 1992.